

## MODELLING OF AIR POCKET ENTRAPMENT DURING PIPE FILLING IN INTERMITTENT WATER SUPPLY SYSTEMS




João P. Ferreira<sup>1</sup>, David Ferras<sup>2</sup>, Dídia I. C. Covas<sup>3</sup>, Zoran Kapelan<sup>4</sup>


<sup>1</sup>Dept. of Water Management, Faculty of Civil Engineering and Geosciences, Delft, Netherlands,

<sup>2</sup>Department of Water Supply, Sanitation and Environmental Engineering, IHE Delft Institute for Water Education, Delft, Netherlands.

<sup>3</sup>CERIS, Instituto Superior Técnico, Universidade de Lisboa, Lisbon, Portugal.

<sup>4</sup>Dept. of Water Management, Faculty of Civil Engineering and Geosciences, Delft, Netherlands,

<sup>1</sup>  [j.p.ferreira@tudelft.nl](mailto:j.p.ferreira@tudelft.nl), <sup>2</sup>  [d.ferras@un-ihe.org](mailto:d.ferras@un-ihe.org), <sup>3</sup>  [didia.covas@tecnico.ulisboa.pt](mailto:didia.covas@tecnico.ulisboa.pt),

<sup>4</sup>  [z.kapelan@tudelft.nl](mailto:z.kapelan@tudelft.nl)

### Abstract

Intermittent water supply (IWS) operations frequently involve water filling and emptying cycles that are strongly influenced by air-water interaction. Storm Water Management Model (SWMM) software has been recently proposed to simulate pipe filling events in IWS systems. As the tool is conceived to simulate both free surface and pressurized flows, it also has the potential to analyse the air entrapment. However, there is no numerical model capable of accurately and efficiently simulating the air behaviour during these events, nor of predicting the locations of air pockets created during the pipe filling process.

An experimental pipe rig was assembled to better understand the pipe filling process in terms of pressure variation, the propagation of the filling wave and the air entrapment locations under different initial conditions. The pipe rig has a classic reservoir-pipe-valve configuration. Different behaviours are observed in this experimental setup during the pipe filling tests. An entrapped air pocket is created at the high point for lower flow rates, which is not dragged when the pipe is full. This air pocket can go from a similarly free surface flow inside the pipe to a complete water filled flow, depending on the flow rate. For low flow rates, a high head loss is introduced due to a hydraulic jump inside the pipe. For higher flow rates, the air is dragged, no air is entrapped and only the local head losses from the change of direction at the high point are observable.

Following the collected experimental data, SWMM is used to assess to which extent it can predict entrapped air pockets location and their volume. Different filling processes can occur and an air model should be included to simulate the tests carried out in the pipe rig. The results obtained show that SWMM is capable of predicting air pocket locations but not the air pocket volumes. Further research is necessary to improve SWMM in this context.

### Keywords

Intermittent water supply, pipe filling, air pockets, experimental test, numerical modelling, SWMM.

## 1 INTRODUCTION

Water supply is of major importance for our daily routines and activities. Water is expected to immediately come out of the taps whenever these are opened by the consumers, giving it the name of continuous water supply (CWS). This assumption is not always true outside of developed countries. Around 40% of the world population is supplied by a piped network that suffers from what is called intermittent water supply (IWS) [1]. Such supply is characterized by a distribution system not being pressurized 24/7, like CWS, with different degrees of reliability. Three different stages can be identified in IWS systems operation: pipe filling, system supply and pipe emptying.

The system starts empty until the utility decides to open valves to start the pipe filling stage. Water goes into the pipe and air needs to be released through taps, tank valves and air valves. However, air can cause severe damage in distribution systems due to unexpected pressure variations in the systems resulting in supply disruptions [2]. Air can compress and expand to the point that it generates pressures that were not accounted for in the design stage, leading to increased pipe failures and higher leakage levels as observed by Christodoulou and Agathokleous [3]. During the filling stage, the system is prone to accumulate entrapped air pockets due to the dynamic behaviour of the flow, but current engineering practice doesn't enable the description of where and under which circumstances air pockets get entrapped other than a rule-of-thumb based on the "high points".

When the pressure is sufficient to deliver water to the service connections, the supply stage starts at that location. The air that was initially in the pipe may or not become entrapped in the system at high points and sudden changes in slope and direction depending on the flow velocity and the pipe slope [4]. Another consequence of having air inside the pipes is the inherent local head losses, due to a reduction of the effective pipe cross section area, which are not negligible in low pressure system due to the high flow velocities as in IWS systems [5, 6]. Thus, air should be released in a controlled way so that lower head losses and pressure variations would occur. However, there is no model to determine air pocket location and volume during/after the pipe filling stage.

The pipe emptying stage begins when the utility closes the connection between the supplying storage tank and the pipe system. Water is still delivered for a short period of time thanks to the reminiscences of pressure in the system and to elevation differences. During this period, air needs to go into the pipes to allow the water flowing out. Either air goes into the pipes by leaks and air valves or sub atmospheric pressures occur in the pipe (in extreme cases leading to pipe buckling). Sub atmospheric pressures are bad not only from the pipe perspective, since they can lead to pipe buckling [7], but also from the water quality perspective, since these allow for losses of untreated water and for contaminants intrusion into the pipe system, putting at risk the supply of safe water [8].

Numerical modelling of water systems can be very useful for predicting air water behaviour during pipe filling and emptying processes. These can be categorized in four types of models: extended period simulation models in pressurized pipes (e.g. EPANET model), free surface flow models in open-pipes (e.g. Stormwater Management Model, SWMM), rigid water column (RWC) model and elastic water column model (EWC).

Extended period simulation models are amply used for pressurized pipes simulation, providing accurate results as long as demands, valves and pumps settings and other boundary conditions are well defined. One of the main assumptions is that the pipes are pressurized 24/7 which is not verified in IWS systems. This assumption also does not make possible to track and detect locations prone to air pocket locations.

Free surface flow models in open-pipes, like SWMM model, has also been used to analyse water systems but in a water drainage perspective. Nevertheless, free surface flows can be accurately

simulated by this model, since the model numerically solves Saint-Venant equations (Eqs. 1 and 2) to calculate water depths:

$$\frac{\delta A}{\delta t} + \frac{\delta Q_w}{\delta x} = 0 \quad (1)$$

$$\frac{\delta Q_w}{\delta t} + \frac{\delta(Q_w^2 / A)}{\delta x} + gA \frac{\delta H}{\delta x} + gAS_f = 0 \quad (2)$$

where  $A$  is the flow cross section,  $Q$  is the water flow rate,  $g$  is the gravitational acceleration,  $S_f$  is the friction factor,  $t$  is time and  $x$  is the length. Specifically using SWMM, the solver features two surcharge methods to when pipes become pressurized: EXTRAN and SLOT surcharge methods. The former relies on mass and momentum equations for pressurized pipes and the second creates an artificial slot on top of the pipe for the assumptions of Saint-Venant equations to remain valid.

Rigid water column models are easy to use and to implement for single pipe systems [9]. Mass continuity and head loss equations are used to estimate flow rates and pressures. Though, the assumptions are incompatible with the existence of entrapped air pockets in the pipes and that of free surface flow existing during the filling process as observed by Guizani *et al.* [10].

Elastic water column models can be applied to pressurized and free surface flows [12, 13] and have been proposed to simulate pipe filling events with water column separation [14]. Accurate results are obtained for both situations. However, lower time steps and higher spatial discretization are required making these models computationally demanding and inefficient for the modelling of pipe networks.

The study of air in pipes has been of interest within the scientific community but with little developments in the IWS domain. Some work has been carried out to determine entrapped air pockets head losses [4] and breakout rates [15] in steady state flows, but such research was never carried for pipe filling events when the dynamic effects are more severe. Also, no hydraulic solver is known to accurately predict air pocket volumes and related pressure variations due to their existence in pipe systems, being such limitation pointed out as one of the main disadvantages of SWMM [16]. SWMM might be used to check the possibility of existence of entrapped air pockets since it simulates open channel flows. Though, since the software was originally developed for drainage purposes, the air pockets are not considered as soon as the cross section prone to air entrapment is pressurized. SWMM has already been suggested as a possible alternative to model IWS systems [11]. Yet, no reference was made to the air behaviour, which is of utmost importance in IWS.

This paper aims at assessing to which extent SWMM can accurately predict air pockets' location and volume in pipe filling events. Experimental results are collected in a laboratory setup to obtain pressure signals and video recordings to better understand the pipe filling process and to determine the air pocket volume. Collected data are compared with numerical results from SWMM to assess if the model can predict the air pocket location and volume.

This paper is organised as follows: section 2 presents the pipe-rig set up and describes the experimental tests that were carried out as well as the conducted test procedure; section 3 summarises the main results from the experimental tests; section 4 briefly explains the numerical model and presents the comparison between numerical and experimental data; and section 5 summarizes the results, presents the main conclusions and further research topics.

## 2 EXPERIMENTAL DATA COLLECTION

### 2.1 Experimental rig



The experimental rig, depicted in Figure 1, is composed of a horizontal acrylic pipe with a horizontal length of 12.4 m and a 21 mm inner diameter. An elevated tank supplies the system and a pneumatically actuated ball valve with an internal diameter of 20 mm controls the pipe filling start at the upstream end of the pipe. A high point is installed at 5.30 m from the upstream valve, having a triangular shaped with a 45° slope with a rising pipe and a downwards pipe in the direction to the downstream end. The height of the high point is 0.30 m. An acrylic plate with a drilled orifice with a diameter  $d = 4.5$  mm was installed to replicate a contraction in the flow cross section at the downstream end of the pipe, just before its discharge into the atmosphere.

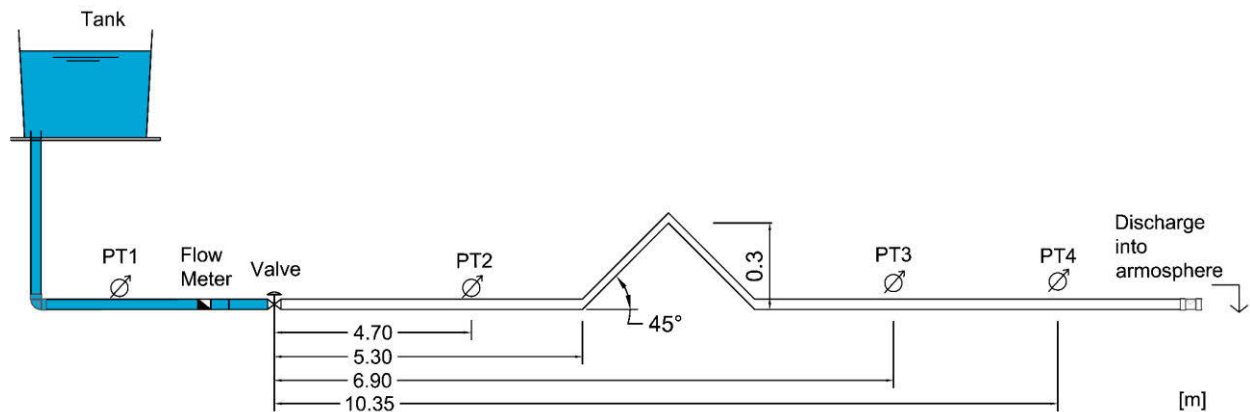


Figure 1. Experimental rig layout

Pressure measurements were carried out using Siemens SITRANS P pressure transducers series Z with a maximum measuring range of 0-2.5 m, a full scale accuracy of 0.5% and a time response lower than 0.1 s. Four pressure transducers were installed in the pipe: (i) the first at the upstream end of the pipe: (i) the first at the upstream end of the valve to control the tank head and used to determine the water tank level as a boundary condition (PT1); (ii) the second (PT2) and the third (PT3) located before and after the system high point at a distance from the upstream valve of 4.7 and 6.9 m, respectively, and (iii) the fourth (PT4) at 10.35 m from the upstream valve. Pressure measurements were acquired at a 1 kHz frequency. Final steady state flow rate measurements were carried out by an Dynasonic ultrasonic flow meter with a full range accuracy of 1%. Video recording were carried out using a GoPro 7 with a resolution of 2074 x 1520 ppx and a frame rate of 24 fps.

## 2.2 Data collection

A number of tests was carried out to estimate the entrapped air pockets volume in the high point of the pipe system. Changing the water tank level and installing an orifice at the downstream end allowed obtaining different filling and final steady state flow rates which resulted in different air pocket sizes. The initial water tank levels,  $H_{ini}$ , were 0.5 and 1.5 m and the two different orifice sizes were tested: one without any orifice and one with the 4.5 mm orifice, corresponding to 10% of the pipe cross sectional area.

Tests are carried out by starting with the pipe completely empty and the orifice to be tested at the downstream end of the pipe. The upstream ball valve is opened and water coming from the tank starts filling the pipe. Air is released from the pipe as the water front wave advances. Once the water front wave reaches the downstream end, a transient is generated since the orifice acts a blockage in the pipe. Once the final steady state is reached (after the transient dissipates), the flow rate is measured. When the test is completed, the pipe is flushed with compressed air to ensure the pipe is emptied for the next test.

### 3 EXPERIMENTAL RESULTS

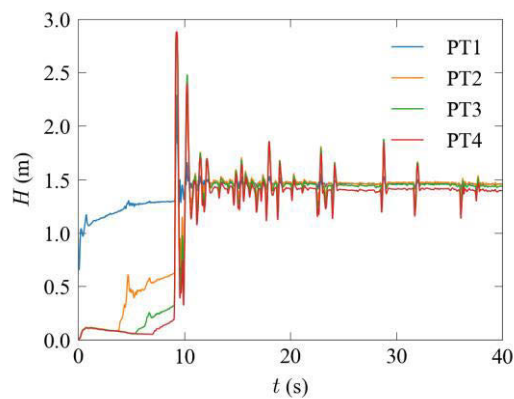
Pressure head, final steady state flow rates and measured air pocket volumes are used to analyse the influence of boundary conditions in air pocket formation. Piezometric head,  $H$ , and resulting steady state air pocket volume are shown in Figure 2 for the  $H_{ini} = 1.5$  m and for the two orifice configurations. Video recordings are analysed to obtain the air pocket volumes,  $V_{air}$  at the final steady state flow. Steady state flow rates and air pocket volumes are presented in Table 1. The higher the flow rate is, the lower the air pocket volume also is, since high flows can drag the air pockets to downstream, as observed by Pothof and Clemens [4].

The measured pressure signal for the downstream configuration with  $d = 4.5$  mm is presented in Figure 2a. A small air pressurization is observed, once the valve opens at time  $t = 0$  s. The air pressurization is equal in all transducers, since the water that enters the system is small comparatively to the pipe volume. The water front wave progresses and reaches each transducer when the pressure signal detaches from the air pressure front the start at  $t = 3.8, 5.4$  and  $7.0$  s for PT2, PT3 and PT4, respectively. PT2 shows a much higher increase in piezometric head when compared to the other transducers, due to the elevation of the high point. When the wave arrives at the downstream end, a pressure variation is observed since the orifice behaves like a blockage and has an inherent local head loss. The steady state piezometric head is progressively lower in the transducers due to head losses. Figure 2b shows the resulting air pocket and there is a clear air pocket formed at the high point.

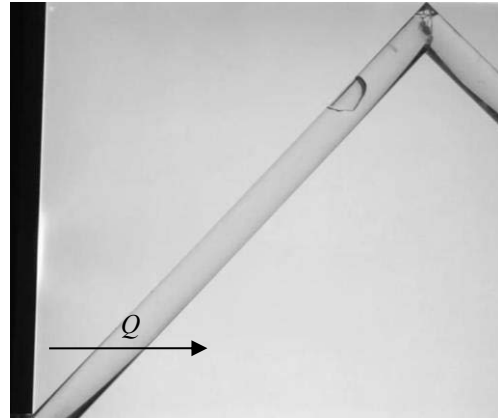
The pressure signal for the downstream configuration with  $d = 21$  mm in Fig 2c does not show any air pressurization since air can be freely released at the downstream end. The water front wave arrives at PT2 at  $t = 3.7$ s and the pressure signal shows the same behaviour as in  $d = 4.5$  mm due to the high point. The wave arrives at PT3 at  $t = 5.2$  s, sooner than in the previous configuration since the air pressurization slightly decreases the filling flow rate, and at PT4 at  $t = 6.4$  s. No pressure variation is observed for this configuration and the piezometric head differences between transducers is much higher due to the higher flow rate presented in Table 1. Figure 2d shows the resulting air pocket for this orifice configuration. The air pocket is considerably smaller and does not create a flow similar to free surface flow on the tipping point of the high point. Even though this air pocket is smaller than the first one, higher head losses are observed due to the higher flow rate as well. Some variability is observed in the air pocket volumes from Table 1 for first and second test tests for the same initial conditions and for  $d = 4.5$  mm.

Table 1. Steady state flow rate and air pocket volume for each tank water level and downstream orifice combination

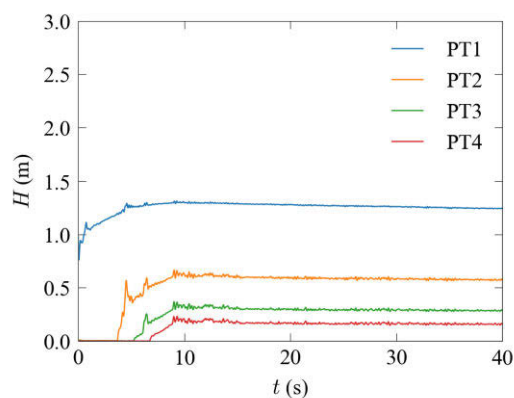
$d$ (mm)		$H_{ini}$ (m)			
		0.5		1.5	
		First test	Second test	First test	Second test
4.5	$Q$ (l/h)	118	90	204	216
	$V_{air}$ (mm <sup>3</sup> )	2246	18181	472	326
21	$Q$ (l/h)	672	666	1263	1232
	$V_{air}$ (mm <sup>3</sup> )	0	0	0	0



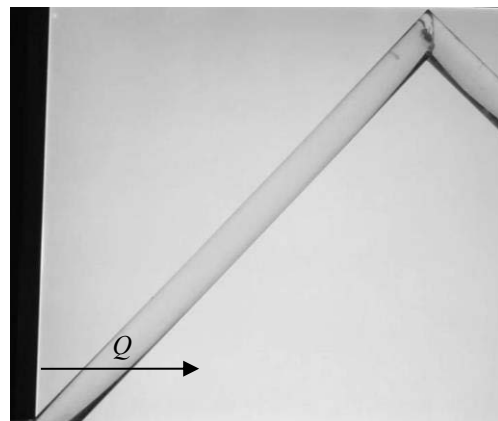
(a)



(b)



(c)



(d)

Figure 2. Pressure signal for each orifice diameter for  $H_{ini} = 1.5$  m and respective air pocket for the orifice configuration of: a, b)  $d = 4.5$  mm and c, d)  $d = 21$  mm

To assess the air pocket volume variability for repeatability purposes, a set of 10 tests was carried out for the configuration  $H_{ini} = 1.5$  m and  $d = 4.5$  mm under the same initial conditions. Figure 3 shows the air pocket volume as a function of the final steady state flow rate. A large variability of air pocket volumes is observed with an average value of  $946 \text{ mm}^3$  and a sampling standard deviation of  $460 \text{ mm}^3$ . However, despite the air pocket volume variability, a consistent flow behaviour is observed in all tests in video recordings: air pockets are always formed at the downwards sloping pipe, slightly after the high point and the flow rate is not capable of clearing the air pocket for this pipe slope. Having this air pocket volume variability, this volume cannot be precisely predicted for a given boundary conditions, but the air pocket location and flow behaviour is expected to be similar. Also, air volumes are estimated based on video records of the tests, thus, there is always some uncertainty in their estimation, though not of the order of magnitude of the observed volume variation.

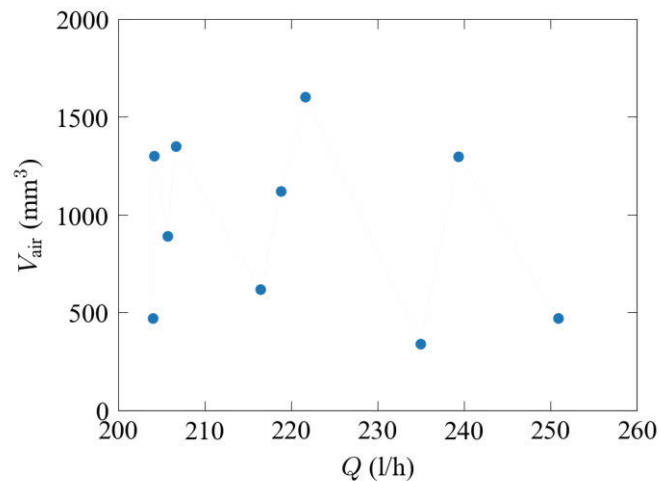


Figure 3. Repeatability analysis of entrapped air pocket volume for  $H_{ini}=1.5$  m and  $d=4.5$  mm

#### 4 SWMM MODEL

The existing SWMM software (v5.1.015) is used to estimate the entrapped air pocket volumes. The model consists of a storage tank at the upstream end, a single pipe simulated by means of pipe sections with a spatial discretization of  $\Delta x = 0.2$  m (to improve dynamic event's results [17]), an orifice at the downstream end of the pipe and a free outfall to simulate the discharge into the atmosphere. Pipe sections from the spatial discretization have a diameter of 0.021 m, are connected to manholes with surcharge depths equal to 100 m so that no node gets ponded [11]. Minimum surface area of the manholes is set to  $1 \times 10^{-5}$  mm<sup>2</sup> to ensure no storage occurs in the manholes. EXTRAN and SLOT surcharge methods included in SWMM are tested. An additional function was added to SWMM source code to track and quantify air pockets' location and volume.

A sensitivity analysis of the spatial discretization was carried out to assess its influence on the simulated air pocket volume in SWMM. For that, the configuration of  $H_{ini} = 0.5$  m and  $d = 4.5$  mm was simulated in SWMM. Simulations for progressively smaller space steps,  $\Delta x$ , in the high point region (0.3 m upwards and downwards) were carried out to determine the value that air pocket volume would converge to, being the remaining pipe with  $\Delta x = 0.3$  m. The spatial steps and the corresponding time steps to ensure stable numerical results are presented in Table 2.

Table 2. Tested spatial discretization and routing time step to assess air pocket volumes

$\Delta x$ (mm)	200	130	100	80	66	57	50	44	40	36	33	31	29	26
$\Delta t$ (ms)	44	29	22	17	14	12	11	9	8	8	7	6	6	5

Numerical results obtained for the air pocket volume for these space steps are presented in Figure 4 for the two surcharge methods. EXTRAN surcharge method results show an increasing air pocket volume until  $\Delta x = 0.05$  m, reaching a maximum value of air volume around  $V_{air} = 25,000$  mm<sup>3</sup> (Figure 4a). SLOT surcharge method results are slightly different, varying from  $V_{air} = 20,000$  and 30,000 mm<sup>3</sup> for space step lower than 0.05 m, but still around the results range for EXTRAN method (Figure 4b). It should be highlighted that the space step that started providing convergent air pocket volume values is four times lower than the recommended by Pachaly *et al.* [17] ( $\Delta x = 0.2$  m) to better describe pipe filling events.

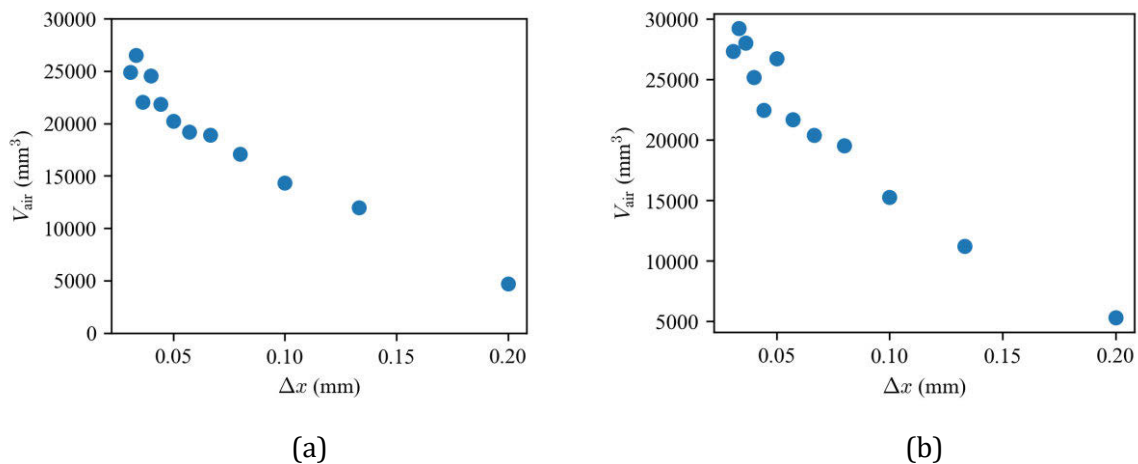


Figure 4. Entrapped air pocket volume for  $H_{ini}=0.5$  m and  $d = 4.5$  mm using: a) EXTRAN and b) SLOT surcharge methods

Tested configurations were simulated in SWMM using a spatial discretization of 0.026 mm, almost ten times lower than the recommended. Table 3 shows the comparison between the SWMM results using EXTRAN surcharge method and the experimental average air pocket volume. Numerical results for  $d = 4.5$  mm do not accurately reproduce experimental data.

Table 3. Experimental vs numerical air pocket volumes for the tested conditions

$d$ (mm)		$H_{ini}$ (m)	
		0.5	1.5
4.5	Experimental $V_{air}$ (mm <sup>3</sup> )	10213	399
	Numerical $V_{air}$ (mm <sup>3</sup> )	25000	19400
21	Experimental $V_{air}$ (mm <sup>3</sup> )	0	0
	Numerical $V_{air}$ (mm <sup>3</sup> )	0	0

However, differences between video recordings and SWMM filling process might explain the difference between air pocket volumes. Figure 5 shows the numerical results from SWMM and an image from the video recording for  $H_{ini} = 1.5$  m and  $d = 4.5$  mm. Figure 5a) presents a snapshot of the pipe filling in SWMM graphic user interface and Figure 5b) shows the air pocket in steady state flow for the aforementioned tested conditions. As observed in Figure 5a), the entrapped air pocket in SWMM is created because the pipe at immediately downstream the high point becomes pressurized. A clear water flow separation occurs between the initial air volume and downstream air volume, leading to the creation of an entrapped air pocket. Video recordings (snapshot in Figure 5b) show a different behaviour: the water filling wave is relatively perpendicular to the pipe cross section and the air pocket only reaches the high point due to air movement when a steady state is reached due to the pressure variations. Thus, the air pocket location is accurately represented in SWMM, but the calculated air volume is much higher than the observed in the experimental tests. Lower flow rates should be tested and an air model should be incorporated in SWMM in order to better describe this filling process and to better quantify the air volume entrapped in the pipe.



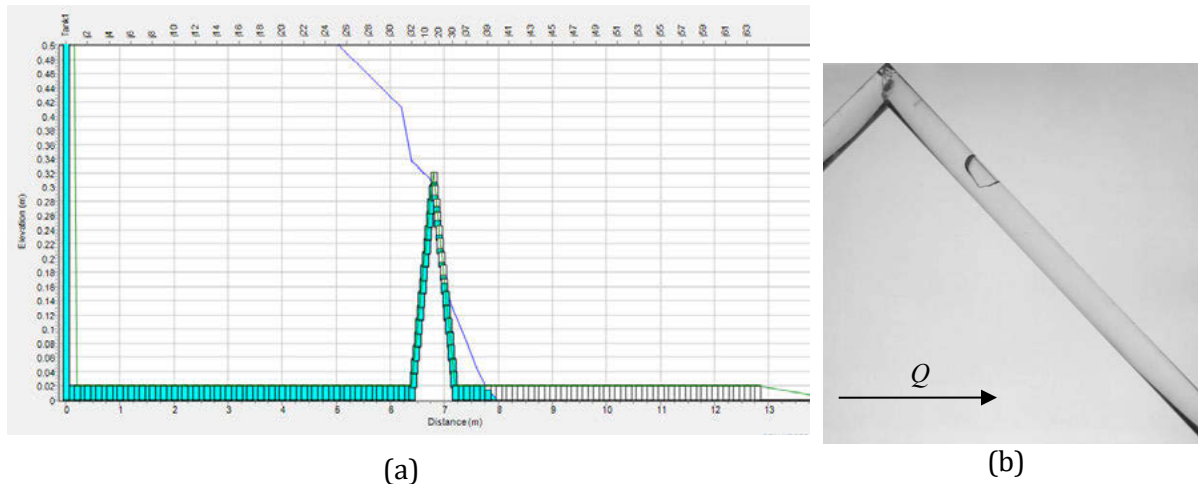


Figure 5. Comparison of air pocket numerically calculated and observed for the test  $H_{ini}=1.5$  m and  $d=4.5$  mm from: a) SWMM pipe filling graphic user interface on the pipe filling process, where blue line is the hydraulic grade line and high point can be observed and b) video recordings

## 5 CONCLUSIONS

Air pockets can compromise the safety of pipe systems upon the occurrence of a transient event. Intermittent water supply systems have a strong air dynamics due to pipe filling and emptying processes. No water supply hydraulic solver is able to accurately describe the phenomena in IWS systems, since these models assume the pipes are already pressurized. SWMM has been proposed as an alternative, since it solves the open-channels equations allowing to simulate pipe filling and emptying stages. However, one of SWMM's main disadvantages is that air pocket dynamic model is not a feature incorporated in the SWMM solver.

This study concludes that, whilst SWMM seems to be able to accurately predict the air pocket location, it is not able to reproduce the air pocket volumes in high sloped pipes. An air model should be incorporated in the SWMM to better estimate the air pocket pressures and volumes. A spatial discretization four times smaller than the recommended in literature was shown to be required to obtain convergent air pocket volumes, but this still requires further research.

## REFERENCES

- [1] B. Charalambous and C. Lapidou Dealing with the Complex Interrelation of Intermittent Supply and Water Losses, 1st Edition, IWA Publishing, 2017.
- [2] L. Ramezani, B. Karney and A. Malekpour, "Encouraging Effective Air Management in Water Pipelines: A Critical Review", *Journal of Water Resources Planning and Management*, vol. 142, no. 12. 2016, pp. 04016055.
- [3] S. Christodoulou and A. Agathokleous, "A study on the effects of intermittent water supply on the vulnerability of urban water distribution networks", *Water Science and Technology: Water Supply*, vol. 12, no. 4. 2012, pp. 523-530.
- [4] I. W. M. Pothof and F. H. L. R. Clemens, "Experimental study of air–water flow in downward sloping pipes", *International Journal of Multiphase Flow*, vol. 37, no. 3. 2011, pp. 278-292.
- [5] I. Pothof and F. Clemens, "On elongated air pockets in downward sloping pipes", *Journal of Hydraulic Research*, vol. 48, no. 4. 2010, pp. 499-503.
- [6] S. Mohapatra, A. Sargaonkar and P. K. Labhassetwar, "Distribution Network Assessment using EPANET for Intermittent and Continuous Water Supply", *Water Resources Management*, vol. 28, no. 11. 2014, pp. 3745-3759.

- [7] Ó. E. Coronado-Hernández, M. Besharat, V. S. Fuertes-Miquel and H. M. Ramos, "Effect of a Commercial Air Valve on the Rapid Filling of a Single Pipeline: a Numerical and Experimental Analysis", *Water*, vol. 11, no. 9. 2019, pp.
- [8] C. M. Fontanazza, V. Notaro, V. Puleo, P. Nicolosi and G. Freni, "Contaminant Intrusion through Leaks in Water Distribution System: Experimental Analysis", *Procedia Engineering*, vol. 119, no. 2015, pp. 426-433.
- [9] J. Parmakian *Water Hammer Analysis*, 1963.
- [10] M. Guizani, J. Vasconcelos, S. J. Wright and K. Maalel, "Investigation of Rapid Filling of Empty Pipes", *Journal of Water Management Modeling*, vol. R225-20,, no. 2006, pp. 463-482.
- [11] A. Campisano, A. Gullotta and C. Modica, "Using EPA-SWMM to simulate intermittent water distribution systems", *Urban Water Journal*, vol. 15, no. 10. 2019, pp. 925-933.
- [12] M. H. Chaudhry *Open-Channel Flow*, 2n Edition, Springer, 2008.
- [13] M. H. Chaudhry *Applied Hydraulic Transients*, 3rd Ed., Springer-Verlag New York, 2014.
- [14] A. Malekpour and B. W. Karney, "Profile-Induced Column Separation and Rejoining during Rapid Pipeline Filling", *Journal of Hydraulic Engineering*, vol. 140, no. 11. 2014, pp. 1-12.
- [15] C. L. Lubbers and F. Clemens, "Breakdown of air pockets in downwardly inclined sewerage pressure mains", *Water Science Technology*, vol. 54, no. 11-12. 2006, pp. 233-40.
- [16] R. L. Pachaly, J. G. Vasconcelos and D. G. Allasia, "Surge predictions in a large stormwater tunnel system using SWMM", *Urban Water Journal*, vol. 18, no. 8. 2021, pp. 577-584.
- [17] R. L. Pachaly, J. G. Vasconcelos, D. G. Allasia, R. Tassi and J. P. P. Bocchi, "Comparing SWMM 5.1 Calculation Alternatives to Represent Unsteady Stormwater Sewer Flows", *Journal of Hydraulic Engineering*, vol. 146, no. 7. 2020, pp. 1-16.